

# Immunolocalization and expression of Na<sup>+</sup>/K<sup>+</sup>-ATPase in embryos, early larval stages and adults of the freshwater shrimp *Palaemonetes argentinus* (Decapoda, Caridea, Palaemonidae)

Romina Belén Ituarte<sup>1</sup> · Jehan-Hervé Lignot<sup>2</sup> · Guy Charmantier<sup>2</sup> · Eduardo Spivak<sup>1</sup> · Catherine Lorin-Nebel<sup>2</sup>

Received: 30 March 2015 / Accepted: 15 December 2015  
© Springer-Verlag Berlin Heidelberg 2015

**Abstract** The euryhaline shrimp *Palaemonetes argentinus* exemplifies an evolutionary transition from brackish to freshwater habitats that requires adequate osmoregulatory capacities. Hyperosmoregulation is functional at hatching and it likely begins during the embryonic phase allowing this species to develop entirely in fresh water. Here, we investigated the Na<sup>+</sup>/K<sup>+</sup>-ATPase  $\alpha$ -subunit gene (*nka- $\alpha$* ) expression using quantitative real-time PCR and localized Na<sup>+</sup>/K<sup>+</sup>-ATPase (NKA) in ion-transporting epithelia through immunofluorescence microscopy. We reared shrimps from spawning to juvenile stages at two salinities (1, 15 ‰) and maintained adults for 3 weeks at three salinity treatments (1, 15, 25 ‰). *nka- $\alpha$*  gene expression was measured in: (1) embryos at an early (SI), intermediate (SII) and late (SIII) stage of embryonic development; (2) newly hatched larvae (Zoea I, ZI); and (3) isolated gill tissue of adults. The *nka- $\alpha$*  expression was low in SI and SII embryos and reached maximum levels prior to hatching (SIII), which were similar to expression levels detected in the ZI.

The *nka- $\alpha$*  expression in SIII and ZI was highest at 15 ‰, whereas salinity did not affect expression in earlier embryos. In SIII, in ZI and in a later zoeal stage ZIV, NKA was localized in epithelial cells of pleurae, in the inner-side epithelium of branchiostegite and in the antennal glands. Gills appeared in the ZIV but NKA immunolabeling of the cells of the gill shaft occurred in a subsequent developmental larval stage, the decapodid. Extrabranchial organs constitute the main site of osmoregulation in early ontogenetic stages of this freshwater shrimp.

**Keywords** Antennal gland · Extrabranchial organs · Gill · Ontogeny · Osmoregulation

## Introduction

Colonization from marine to freshwater environments is considered one of the most dramatic evolutionary transitions in the history of life (Lee and Bell 1999; Miller and Labandeira 2002; Lee et al. 2011, 2012). Although crustaceans are the most frequently invertebrates reported as recent freshwater invaders (e.g., Lee and Bell 1999; Johnson et al. 2014), few species of decapods (crabs, crayfishes and shrimps) have successfully adapted to fresh water: only about 1000 among the approximately 10,000 known species are able to spend their entire life cycle at constantly low salinity (Anger 2001). Life in fresh water requires the ability to actively transport (uptake) essential ions from dilute environments, which is energetically costly because organisms must regulate their body fluids against important ion concentration gradients. Such regulatory functions are energetically driven by ion-motive ATPase enzymes, such as Na<sup>+</sup>/K<sup>+</sup>-ATPase and V-type H<sup>+</sup>-ATPase, which have been hypothesized to be critical for the colonization of fresh water in

**Electronic supplementary material** The online version of this article (doi:10.1007/s00441-015-2351-0) contains supplementary material, which is available to authorized users.

✉ Romina Belén Ituarte  
ituarte@mdp.edu.ar

<sup>1</sup> Grupo Zoología Invertebrados, Instituto de Investigaciones Marinas y Costeras, Consejo Nacional de Investigaciones Científicas y Técnicas (CONICET), Universidad Nacional de Mar del Plata, Dean Funes 3250, 7600 Mar del Plata, Argentina

<sup>2</sup> Groupe Fonctionnel Adaptation Ecophysiologique et Ontogenèse, UMR 9190 MARBEC, UM-CNRS-IRD-Ifremer, Université Montpellier, cc 092, Place E. Bataillon, 34095 Montpellier cedex 05, France

several decapods (e.g., Weihrauch et al. 2001, 2004; Lee et al. 2011; Boudour-Bouchecker et al. 2014; Lucena et al. 2015; Maraschi et al. 2015).

Hyper-osmoregulation in dilute media occurs in several decapod taxa including shrimps and this ability is generally present early in the ontogeny, i.e., during larval or even embryonic stages, especially in fresh water (Charmantier 1998; Anger 2001). Particular attention has been paid to the strong ability of Decapoda to osmoregulate thanks to their branchial chamber including gills and branchiostegites (reviewed in Charmantier et al. 2009; McNamara and Faria 2012; Lignot and Charmantier 2015). The ontogeny of osmoregulatory capacity and salinity tolerance are frequently linked to the development of ion-transporting cells (ionocytes) in these organs (Charmantier et al. 2009; Boudour-Bouchecker et al. 2013). These cells express a pool of transmembrane proteins, such as  $\text{Na}^+/\text{K}^+$ -ATPase, one of the main driving enzymes involved in the process of active transepithelial ion exchanges (Péqueux 1995; Charmantier 1998; Lucu and Towle 2003; Charmantier et al. 2009). As ion-transporting epithelia may change during development,  $\text{Na}^+/\text{K}^+$ -ATPase has been localized to reveal the presence or absence of ionocytes. Precise information about the subcellular location of ion-transporting cells is available mainly for adult decapods (Péqueux 1995; Charmantier 1998; Lucu and Towle 2003; Charmantier et al. 2009), less frequently for larvae (Felder et al. 1986; Cieluch et al. 2005, 2007; Boudour-Bouchecker et al. 2013) and scarcely at all for embryos (Khodabandeh et al. 2006). Temporary or exclusive ion-transporting organs may be functional during embryonic life (Charmantier and Charmantier-Daures 2001; Seneviratna and Taylor 2006) but the osmoregulatory capacity of decapod embryos has not been closely linked to embryonic organs until recently (Lignot and Charmantier 2001; Seneviratna and Taylor 2006). Instead, salinity tolerance in decapod embryos has been mostly related to the permeability of the egg membranes (Robertson 2013).

The euryhaline shrimp *Palaemonetes argentinus* (Nobili 1901) is widely distributed in brackish coastal lagoons connected to the sea but also in inland lakes and streams, geographically ranging from central eastern Argentina to Uruguay and southern Brazil. This species has a complex life cycle with benthic adult and juvenile stages and a planktonic phase including at least 7 zoeae and several decapodid stages of increasing structural complexity (Menú-Marque 1973; Anger 2001). Such an extended larval development is common in palaemonid species from marine habitats and may indicate a recent evolutionary transition to fresh water (Anger 2001). In fact, this species is able to complete its entire life cycle in freshwater or brackish conditions ranging from about 1 to 25 ‰ but the existence of wild populations confined to land-locked habitats with very low salinities suggests that larval development does not depend on brackish water (Ituarte et al. 2005; Ituarte 2008; Ituarte et al. 2010). Its entire development in fresh water is possible thanks

to efficient hyperosmoregulation of all postembryonic developmental stages (Charmantier and Anger 1999).

In *Palaemonetes argentinus*, as in other decapods, the gills are enclosed in a pair of branchial chambers formed by the pleurae and lateral extensions of the tergum, the branchiostegites. This species has typical palaemonid phyllobranchiate gills (Sousa and Petriella 2005) that are supposed to be the major osmoregulatory organ in the adult stage (Charmantier and Anger 1999). Besides the gills, other specialized tissues from the adult branchial chambers along with excretory antennal glands have also been suggested to be involved in the strong ability of this shrimp to hyperosmoregulate in dilute media (Charmantier and Anger 1999). Despite these assumptions, the ontogeny of ion-transporting tissues/organs has not so far been studied in this species. Moreover, whether the ability to hyper-osmoregulate is already developed at some point during embryogenesis is still unknown due to technical problems of sampling the hemolymph from small crustacean embryos. However, a substantial increment in the specific activity of  $\text{Na}^+/\text{K}^+$ -ATPase has been detected after transfer to high salinities (15 and 25 ‰), not only in adult gills but also in first larvae and in late embryos, suggesting that mechanisms typically found in euryhaline adults (i.e., active ion transport based on  $\text{Na}^+/\text{K}^+$ -ATPase activity) are functional in early life-history stages (Ituarte et al. 2008). Therefore, we hypothesize that the function of hyper-osmoregulation is already present at some point during embryonic development, most probably during the final phase of embryogenesis, as in crayfish (Susanto and Charmantier 2000, 2001).

In the present study, we immunostained  $\text{Na}^+/\text{K}^+$ -ATPase (NKA), as an indicator for tissues with high active ion-exchange capacities, in selected developmental stages: late embryos, first and intermediate zoeal stages, first decapodid (= transition stage between larvae and juveniles), the first juvenile and the adult of the palaemonid shrimp *Palaemonetes argentinus*. In addition to immunohistochemical staining, we quantified the relative amount of  $\text{Na}^+/\text{K}^+$ -ATPase  $\alpha$ -subunit transcripts (*nka- $\alpha$* ) during embryonic development and after hatching (first larvae and adults) by means of real-time quantitative polymerase chain reaction (qPCR), a powerful technique for profiling gene expression. Therefore, in this study, we gathered information on *when* NKA appears and *where* ion-transporting tissues/organs are located throughout development of the freshwater shrimp *P. argentinus*.

## Materials and methods

### Animals

Adult *Palaemonetes argentinus* were collected in Lake Chascomús (35°36'S, 58°W), Argentina in October and November, 2012 (for more details of the habitat, see Ituarte et al.

2010). Shrimps were transported to the laboratory, where they were sorted into two groups: (1) females without eggs or developed ovaries, which were selected as adult stage for experimentation and (2) females with fully developed ovaries that were kept together with males until ovigerous females appeared, which were then isolated for experimentation. Prior to experiments, the animals were housed in 30-L aquaria in 15 L of dechlorinated tap water, with oxygen supply, at  $22 \pm 2$  °C and 14:10 h L:D photoperiod, for 7 days. TetraMin Pro® Tropical Crisps was provided daily as food. Adult shrimps were always directly transferred from dechlorinated tap water to 1 ‰ and 15 ‰, or acclimated for approximately 1 h at 15 ‰ until reaching 25 ‰. Water was obtained by dilution of filtered seawater (Schleicher and Schuell filter paper 0859, pore size ca. 7–12 µm) with dechlorinated tap water and UV disinfection. Culture conditions during experimentation (temperature, photoperiod and food) were the same as described above for all developmental stages.

**Adults** Shrimp were kept at three different salinities: 1, 15 and 25 ‰ for at least 3 weeks in 15-L aquaria. Water was partially changed (70 %) once a week.

**Ontogeny** Females with newly fertilized eggs (= embryos) were kept individually in 2-L aquaria at two salinity treatments, 1 and 15 ‰. Water was partially changed (70 %) once a week. Total embryonic development from spawning of embryos to hatching took between 18 and 24 days. Embryos were carefully detached from each female at three development stages (on days 2, 10 and 18 from spawning, called SI, SII and SIII) using a stereomicroscope. The three stages of embryonic development (SI, SII, SIII) used in this study correspond to those described by Ituarte et al. (2008).

Immediately after larval release, newly hatched larvae (Zoea I, ZI) of each female were collected with a plastic pipette for molecular analysis (see below). Another subset of newly hatched larvae were individually reared in plastic beakers (50 ml) filled with water at the same salinity and culture conditions as during embryonic development. Water and food (newly hatched *Artemia* spp nauplii) were changed daily. The complete larval development from hatching to juvenile stage took between 38 and 42 days. Molting was checked every day. The zoeal stages I and IV, the first decapodid=postembryonic instar VIII (D) and the first juvenile (J) were selected for histological preparations.

### Molecular biology

Whole embryos (SI, SII, and SIII), entire larvae (ZI) and adult shrimps were immediately preserved in RNAlater® (Ambion), stored at 4 °C overnight and frozen at –20 °C. Ten replicates for each developmental stage and salinity treatment (1 and 15 ‰) with 40–100 embryos and 30–80 ZI per

replicate were taken from 80 different females. Gills were removed with sterile tweezers from both the left and right sides of the branchial chamber of 10 adult shrimps per salinity treatment (1, 15 and 25 ‰) before RNA extraction.

### RNA purification and first-strand synthesis of cDNA

Total RNA was extracted from whole embryos and larvae but from individually dissected gills (adults) using the Trizol® reagent (Ambion®; Invitrogen) according to the manufacturer's instructions and quantified using a NanoDrop® ND-1000 V3300 Spectrophotometer (Nanodrop Technology, Wilmington, DE, USA). The A260/A280 ratio of purified RNA ranged from 1.76 to 2.06. Total RNA (1 µg) was treated with RNase-free DNase (Invitrogen) and the reverse transcription was performed using M-MLV reverse transcriptase (Invitrogen) and random primers (Invitrogen). The resulting cDNA was stored at –20 °C until use.

### Primer design

**Na<sup>+</sup>/K<sup>+</sup>-ATPase α subunit** The putative Na<sup>+</sup>/K<sup>+</sup>-ATPase α subunit from *Palaemonetes argentinus* was amplified by PCR using degenerated primers dNKA-F and dNKA-R (Table 1), which were designed based on nucleotide BLAST alignments of the NKA α subunit from different crustacean species: *Callinectes sapidus* (GenBank accession no. AF327439.1), *Eriocheir sinensis* (AF301158.1), *Fenneropenaeus indicus* (HM012803.1), *Macrobrachium amazonicum* (GQ329698.1), *Macrobrachium rosenbergii* (EU427176.1) and *Pontastacus leptodactylus* (DQ834382.1).

**Elongation Factor 1- α1 (ef1-α1)** Degenerated primers dEF1-F and EF1-R (Table 1) were designed based on nucleotide BLAST alignments of the *ef1-α1* from 8 different species including *Saccharomyces cerevisiae* (M10992), *Alpheus thomasi* (AF310826.1), *Daphnia magna* (AB734039.1), *Litopenaeus vannamei* (GU136229.1), *Palaemonetes varians* (FJ654544.1), *Danio rerio* (DQ083545.1), *Mus musculus* (NM\_010106.2) and *Homo sapiens* (NM\_001402.5). All sequences were aligned with the application ClustalW Multiple Alignment using BioEdit Sequence Alignment Editor v.7.2.0. Conventional polymerase chain reaction (PCR) was performed on template cDNA (1 µl cDNA corresponding to 48 ng RNA equivalent) using GoTaq® Flexi DNA Polymerase (Promega) following the manufacturer's instructions. PCR conditions consisted in a 2-min initial denaturing step at 95 °C, followed by 35 cycles of 1 min denaturation at 95 °C, 1 min annealing at 55 °C (for degenerated primers) and 1 min extension at 72 °C, as well as a final extension step of 5 min at 72 °C. PCR products were checked by electrophoresis. Degenerated primers amplified a 589-bp and a 495-bp fragment for NKA and EF1, respectively. PCR products were

**Table 1** *Palaemonetes argentinus* nucleotide sequence of degenerate (*d*) and specific (*s*) primers used for conventional and real-time quantitative PCR amplification of Na<sup>+</sup>/K<sup>+</sup>-ATPase  $\alpha$ -subunit (NKA) and Elongation Factor 1- $\alpha$ 1 (EF1- $\alpha$ 1)

Target genes	Primer name	Sequence (5' to 3')	Amplicon length (base pairs)
NKA	dNKA-F	GACAAYACCATYATYGARGC	589
	dNKA-R	STCYATGATYGAYCCBCCHM	
	sNKA-F	GAACTGGATGAGGAAATGAAG	115
	sNKA-R	AGGGGGTATTTGTCAGAAGG	
EF1- $\alpha$ 1	dEF1-F	GARTTYGARGCYGGTATCTC	495
	dEF1-R	GGGCACWGTWCCAATACCWCC	
	sEF1-F	CCTGGTGAAGAAGAAGAAG	106
	sEF1-R	TTGTCTGTAGGTCTGGATGG	

Nucleotide code: Y = C/T; R = A/G; K = G/T; D = A/G/T; V = A/C/G; S = S/G; W = A/T

purified with a QIAquick PCR purification kit (Qiagen) and directly sequenced at the Génotypage-Séquençage platform of IFR 119 (Montpellier, France) with an ABI Prism 3130 XL 16 capillary Genetic Analyzer instrument (Applied Biosystems).

A nucleotide blast (using the NCBI database) of the *nka- $\alpha$*  subunit partial sequence of *Palaemonetes argentinus* (GenBank accession no. KJ443692) generated a high nucleotide identity with other *nka- $\alpha$*  subunits of numerous shrimp species ranging mostly from 90 to 95 % with a query cover ranging from 95 to 100 %. For *efl- $\alpha$ 1* (KJ443693), the blast showed a nucleotide identity of 77 to 82 % with *efl- $\alpha$*  sequences of several crustacean species such as *Gammarus balcanicus*, *Cancer borealis*, *Marsupenaeus japonicus* and *Alpheus immaculatus* with a query cover ranging from 58 to 100 %. From these partial sequences, we designed specific primers sNKA-F; sNKA-R; sEF1-F and sEF1-R (Table 1) used in real-time quantitative PCR. These primers amplified a PCR product of 115 bp for *nka- $\alpha$*  and 106 bp for *efl- $\alpha$ 1* and their specificity was tested by electrophoresis.

#### Quantification of mRNA expression by real-time quantitative PCR (qPCR)

Real-time quantitative polymerase chain reactions (qPCR) were performed with a thermocycler LightCycler™ 480 (Roche, Mannheim, Germany) using 2.5  $\mu$ L of the SYBR-Green I Master Mix (Roche), 0.5  $\mu$ M of the specific primers and 1  $\mu$ L of cDNA (corresponding to 0.75 ng of RNA equivalent for embryos and larvae and 1.5 ng for adult gills). The cycling qPCR conditions consisted in a 5-min initial denaturation step at 95 °C, followed by 45 cycles of 10 s amplification at 95 °C, 10 s annealing at 60 °C and 10 s extension at 72 °C. Then, a melting curve was generated for 5 s at 95 °C and 1 min at 65 °C and a final cooling step of 30 s at 40 °C in order to check for each primer set if the PCR product is free of non-specific by-products. The results were normalized with the elongation factor *efl- $\alpha$ 1*, a housekeeping gene that did not change according to salinity or developmental stages (see “Results”). Water instead of cDNA was used as a no-

template negative control in the qPCR. Dilution series of a cDNA mixture of several analyzed samples were performed in order to generate a standard curve and to determine the efficiencies of each primer pair (1.875 for *nka- $\alpha$*  and 1.95 for *efl- $\alpha$ 1*). The relative expression of NKA in each stage was calculated using the LightCycler 480 (Roche) advanced relative quantification method (e.g., E-Method) with the respective efficiencies and using a standard in each run.

#### Histological preparations and immunohistochemical localization of Na<sup>+</sup>/K<sup>+</sup>-ATPase

Samples of embryos (SI, SII, SIII), larvae (ZI, ZIV, D), juveniles (J) and adults (A) were fixed for 24 h in Bouin's liquid. After rinsing in 70 % ethanol, samples were fully dehydrated in an ascending series of ethanol (90 and 100 %). After impregnation in butanol, histochoice clearing agent (Amersco, USA) and Paraplast (Sigma-Aldrich, USA), the samples were embedded in Paraplast. Transverse and longitudinal sections (4  $\mu$ m thick) were cut on a Leitz Wetzlar microtome, collected on poly-L-lysine-coated slides and stored at 38 °C for 48 h. Dry slides were used for classic light microscopy with Masson's Trichome staining for tissue observation on a Leica Diaplan light microscope.

#### Immunohistochemical localization of Na<sup>+</sup>/K<sup>+</sup>-ATPase

The slides were deparaffinized in Histochoice tissue solution (Sigma) for 10 min, washed in butanol and hydrated through a descending alcohol series (100, 95, 90, 70 and 50 % for 5 min each). The slides were incubated for 10 min in a mixture of 0.01 % Tween 20, 150 mM NaCl in 10 mM phosphate-buffered saline (PBS), pH 7.3. Subsequently, sections were incubated for 20 min in a solution of 5 % skimmed milk powder (SMP)/PBS to block non-specific binding. The primary antibody, a rabbit polyclonal antibody raised against an internal region of Na<sup>+</sup>/K<sup>+</sup>-ATPase  $\alpha$ 1 of human origin [Na<sup>+</sup>/K<sup>+</sup>-ATPase  $\alpha$  (H-300); Santa Cruz Biotechnology] was diluted in 0.5 % SMP/PBS to 10  $\mu$ g/ml and incubated for 2 h at

room temperature in a wet chamber. The specificity of this antibody has been tested previously by western blot in the shrimp *Macrobrachium amazonicum* (Boudour-Bouchecker et al. 2013). To remove unbound antibodies, the sections were washed ( $3 \times 5$  min) in PBS and then incubated with the secondary antibody (AlexaFluor 488 goat anti-rabbit IgG; Invitrogen) at  $10 \mu\text{g/ml}$  in 0.5 % SMP/PBS for 1 h at room temperature. Control slides were exposed to the same conditions without primary antibody (negative control). Slides were mounted in an anti-bleaching mounting medium (Gel/Mount; Permanent Aqueous Mounting, Biomeda, Plovdiv, Bulgaria), observed with a Leica Diaplan microscope equipped with the appropriate filter set (450–490 nm) and photographed with a Leica DC 300 F digital camera coupled to FW4000 software for photodocumentation (Leica Microsystems, Reuil-Malmaison, France).

### Image analysis procedure

Serial transverse sections of whole individuals were made for each one of the following developmental stages and salinity treatments:  $n = 3$  adults,  $n = 5$  juveniles,  $n = 5$  decapodids,  $n = 4$  zoeae IV and  $n = 4$  zoeae I. Similar sections from the cephalothoracic region from each developmental stage were selected for a semi-quantitative analysis of fluorescence. Gills and branchiostegites were analyzed separately. Sections were photographed under the magnification  $\times 40$ , always using the same setting parameters (aperture, exposure time and exposure compensation) determined at the beginning of the analyses. A single microphotograph of the gills contained at least four lamellae, thus we measured four fluorescence values, one per each lamella (Electronic Supplementary Material, Fig. S1). Moreover, we photographed three different regions (parts) of branchiostegites to obtain three fluorescence values from this epithelium for each individual. Fluorescence was quantified using ImageJ 1.48 software. Digital images were converted to a gray scale, the edge of either tissue was selected with the polygon tool and the following measurements were obtained: area, integrated density and mean gray value. A region without fluorescence located next to the selected tissue was used as background reading (further details in Electronic Supplementary Material, Fig. S2). Corrected total fluorescence (CTF) was analyzed with the formula:  $\text{CTF} = \text{integrated density} - (\text{area of selected tissue} \times \text{mean fluorescence of background readings})$  modified from <http://sciencetechblog.files.wordpress.com/2011/05/measuring-cell-fluorescence-using-imagej.pdf> (Electronic Supplementary Material, Fig. S3).

### Scanning electron microscopy

Branchial chambers from adults held at 1 ‰ were maintained in 70° ethanol and dehydrated through an ethanol series and a 1,1,1,3,3,3-hexamethyldisilazane bath. After being air-dried,

samples were observed with a Quanta FEG 200 (FEI, The Netherlands) equipped with an X-MAX EDS detector (Oxford Instruments).

### Statistical analysis

All values were expressed as arithmetic mean  $\pm$  standard deviation (SD). Statistical analysis of the data was performed using SigmaStat 3.5 software. Differences in mRNA transcript abundances and in corrected total fluorescence (CTF) between life-history stages and salinity treatments were tested by 2-way ANOVAs and Tukey tests for post hoc pairwise multiple comparisons. Differences in gill mRNA levels and in CTF from adult tissues among salinities (1, 15 and 25 ‰) were analyzed by one-way ANOVAs and Student–Newman–Keuls tests. All tests were performed after checks for normal distribution and equality of variance;  $P < 0.05$  was used to assess statistical significance.

## Results

### Ontogeny of osmoregulatory structures and immunolocalization of NKA

The ontogeny of osmoregulatory structures was analyzed in embryonic stages SI, SII and SIII; zoeal stages I and IV; decapodids; juveniles and adult shrimps. The high percentage of yolk in early embryonic developmental stages (SI, SII) did not allow good quality sectioning.

#### Branchial chamber

**Adults** The general organization of the branchial chamber in adult *P. argentinus* is shown in Fig. 1a, c. Each branchial chamber contains seven phyllobranchiate gills and two small epipodites (Fig. 1c). Higher magnification images of a phyllobranchiate gill, an epipodite and a part of branchiostegite are shown in Fig. 1b, d–f. No apparent difference in structure was notable between the different lamellae along the gill axis or between the anterior and posterior gills. Strong NKA immunostaining was observed in the inner epithelium of branchiostegites (Fig. 2c), in the central part of lamellae of the seven gills (Fig. 2a, b) and in the two facing epithelia of epipodites (Fig. 2d). Control sections without the primary antibody showed no immunolabeling (not shown).

**Ontogeny** Late embryonic stage (SIII) and first zoeae (ZI) of *P. argentinus* showed strong immunostaining along the inner epithelium of branchiostegite and in the epithelial cells of pleurae (Fig. 3a, c). We did not observe any gill or epipodite in these early developmental stages. In the zoea IV, the inner

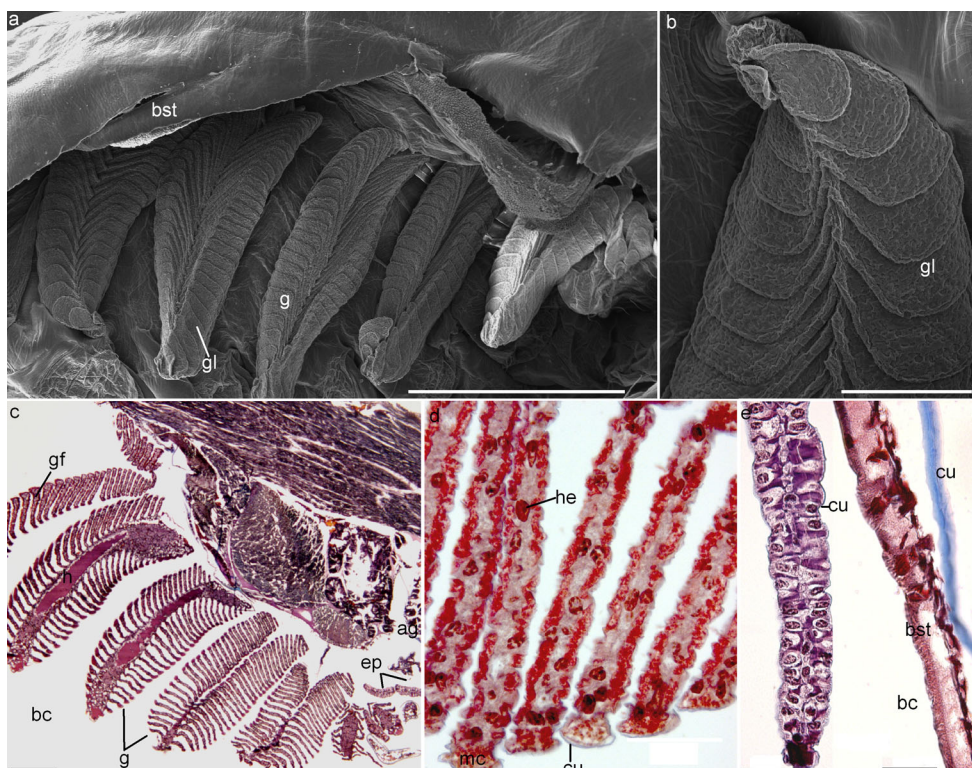


**Fig. 1** Branchial chamber of adult *Palaemonetes argentinus* kept at 1 ‰. Scanning electron micrographs **a**, **b**. **a** The right gill chamber with branchiostegite partly removed to show the phyllobranchiate gills; **b** higher magnification of the gills showing the double row of gill lamellae on either side of the gill axis characteristic of phyllobranches. **c** Fully developed gills in the branchial chamber. **d** Higher magnification of the gill lamellae. **e** Epipodite. **f** Vertical longitudinal section of the

branchiostegite. **c**, **d**, **e** Longitudinal sections. *ag* antennal gland; *bc* branchial chamber; *bst* branchiostegite; *cu* cuticle (**f**: cuticle detached from the branchiostegite epithelium); *ep* epipodite; *g* gill; *gf* gill filament; *gl* gill lamellae; *gs* gill shaft; *h* hemolymph; *he* hemocyte; *mc* marginal canal with hemolymph. Scale bars (**a**) 1 mm; (**b**) 150  $\mu$ m; (**c**) 300  $\mu$ m; (**d–f**) 50  $\mu$ m

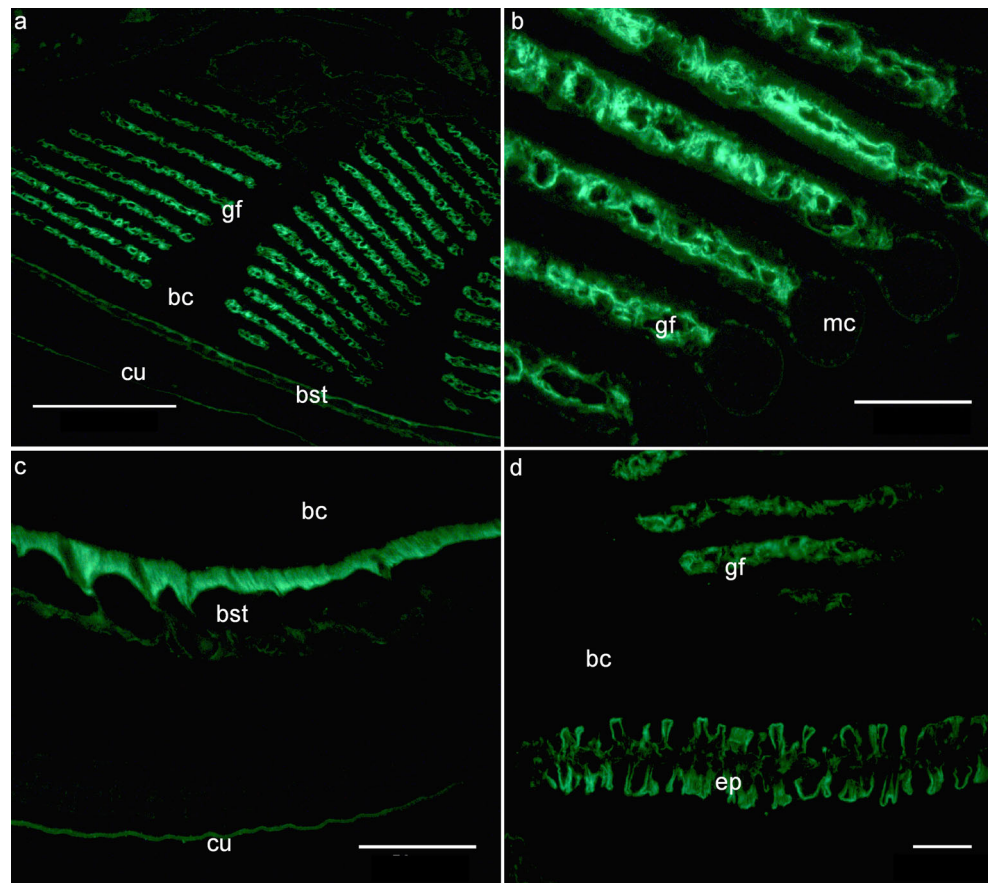
epithelium of branchiostegite and epithelial cells of the pleurae also showed positive immunoreactivity for NKA. Incipient gill lamellae were observed at this stage (Fig. 3f) but they were not immunostained. Immunofluorescence in gill lamellae was observed for the first time in the decapodid (Fig. 3g), but it disappeared from pleurae at this stage. In decapodids reared at 15 ‰, stronger immunostaining was observed in the inner epithelium of branchiostegite as compared with both earlier zoeal stages (Fig. 5a; see also below). In juveniles, the inner epithelium of branchiostegite was strongly immunostained, without showing significant intensity differences between salinity treatments (Fig. 5a; see also below). The central part of the gill lamellae of juveniles was immunostained without differences between salinities (Fig. 5b; see below) and the two facing epithelia of epipodites showed positive immunolabeling (not shown).

#### Antennal glands

Two antennal glands were observed in the zoea I, ventrally on both sides of the central nervous system; they were

immunostained for NKA (Fig. 3d). These glands were already developed from the late embryonic stage (SIII; Fig. 3b) and in both life-history stages they showed simple tubule-like structures without morphologically distinguishable regions (Fig. 3b, e). This tubule showed stronger immunostaining at 15 ‰ than 1 ‰ in zoea I (not shown). As in the previous life-history stages, the tubule did not show any morphological differentiation in zoea IV and decapodid; however, in the decapodids, its basal side showed stronger immunofluorescence than the apical part (Fig. 4a, b). Moreover, two regions were recognized in the decapodid gland: bladder and tubule; immunostaining was stronger in the bladder than in tubule cells (Fig. 4b). In juveniles, there was an increase in the size of the glands and in the folding of the tubules (Fig. 4c). Glands of juveniles and adults showed immunolabeling in all three regions: bladder, proximal and distal tubules (Fig. 4d–f) and immunostaining was stronger in the proximal than in the distal tubule (Fig. 4d). As in the decapodid stage, immunostaining was stronger in bladder cells than in the tubule (Fig. 4c–e). Moreover, NKA staining appeared localized throughout cells of the bladder, while it seemed more concentrated on the basal part of the cells of the proximal tubules (Fig. 4e, f).

**Fig. 2** Immunolocalization of  $\text{Na}^+/\text{K}^+$ -ATPase in organs of the branchial chamber from adult *Palaemonetes argentinus* maintained in 1 ‰ for 3 weeks. **a** Gills and branchiostegite. **b** Gill lamellae. **c** Branchiostegite. **d** Epipodite. Abbreviations, see Fig. 1. Scale bars (**a**) 300  $\mu\text{m}$ ; (**b–d**) 50  $\mu\text{m}$



## Semi-quantitative analyses

### Branchial chambers

**Adults** The NKA-corrected total fluorescence (CTF) in both gill and branchiostegite epithelia was significantly affected by salinity (gill:  $F_{2, 35} = 54.2$ ;  $P < 0.01$ ; branchiostegite:  $F_{2, 26} = 28.31$ ;  $P < 0.001$ ). In both tissues, the highest values occurred at 1 ‰, intermediate ones at 15 ‰ and the lowest values at 25 ‰ (Fig. 5a, b; Student-Newman-Keuls,  $P < 0.05$ ).

**Ontogeny** The inner epithelium of branchiostegite showed strong immunostaining from SIII embryos (Fig. 3a, c, g) until the adult stage (Fig 2c). The SIII stage was not included in semi-quantitative analyses due to technical problems: it was not possible to consistently obtain the same position for sectioning. At each salinity level, the CTF of branchiostegite changed significantly across life-history stages ( $F_{4,113} = 8.4$ ;  $P < 0.001$ ; Fig. 5a). At the low salinity (1 ‰), there was no difference in immunostaining among larval developmental stages (ZI, ZIV and D), while a significant increase occurred in juveniles, reaching a maximum immunostaining in adult shrimps (Fig. 5a). At 15 ‰, ontogenetic patterns of CTF differed from those observed at 1 ‰ (Fig. 5a). Higher salinity

during the whole development (15 ‰) induced differences in the CTF of branchiostegites ( $F_{1,113} = 26.5$ ;  $P < 0.001$ ); however, there was also a significant interaction between salinity and life-history stages ( $F_{4,113} = 23.3$ ;  $P < 0.001$ ). This interaction was due to the fact that salinity induced high NKA expression in the larval stages (ZI, ZIV, D) but the opposite pattern was detected in adults (Fig. 5).

Although gills were present from the ZIV, they did not show NKA immunostaining until the decapodid stage (Fig. 3f, g). NKA immunostaining of the gill tissue changed significantly across life-history stages ( $F_{2,103} = 36.6$ ;  $P < 0.001$ ), between salinities ( $F_{1,103} = 13.8$ ;  $P = 0.003$ ) and there was no interaction between factors ( $F_{2,103} = 1.8$ ;  $P = 0.17$ ). At both salinity treatments, immunostaining increased significantly from decapodid to adult stages (Fig. 5b; Tukey,  $P < 0.05$ ). The CTF in gills from adults was stronger at 1 ‰ than 15 ‰, whereas it was not affected by salinity in decapodid and juvenile stages.

### $\text{Na}^+/\text{K}^+$ -ATPase $\alpha$ -subunit mRNA expression

**Adults** The partial sequences (*nka- $\alpha$*  and *ef1- $\alpha$ 1*) from *Palaemonetes argentinus* showed a high percentage of identity with those from other crustaceans and even insects, indicating that both are highly conserved sequences. There was no

**Fig. 3** Immunolocalization of  $\text{Na}^+/\text{K}^+$ -ATPase in early life-history stages of *Palaemonetes argentinus* developed in 1 ‰. **a, b** Embryo near hatching (SIII). **c–e** Zoea I stage (ZI). **f** Zoea IV stage (Masson staining). **g** Decapodid stage. *p* pleura; *t* tubule; more abbreviations, see Fig. 1. Scale bars: (**a–c, e–g**) 50  $\mu\text{m}$ ; (**d**) 300  $\mu\text{m}$

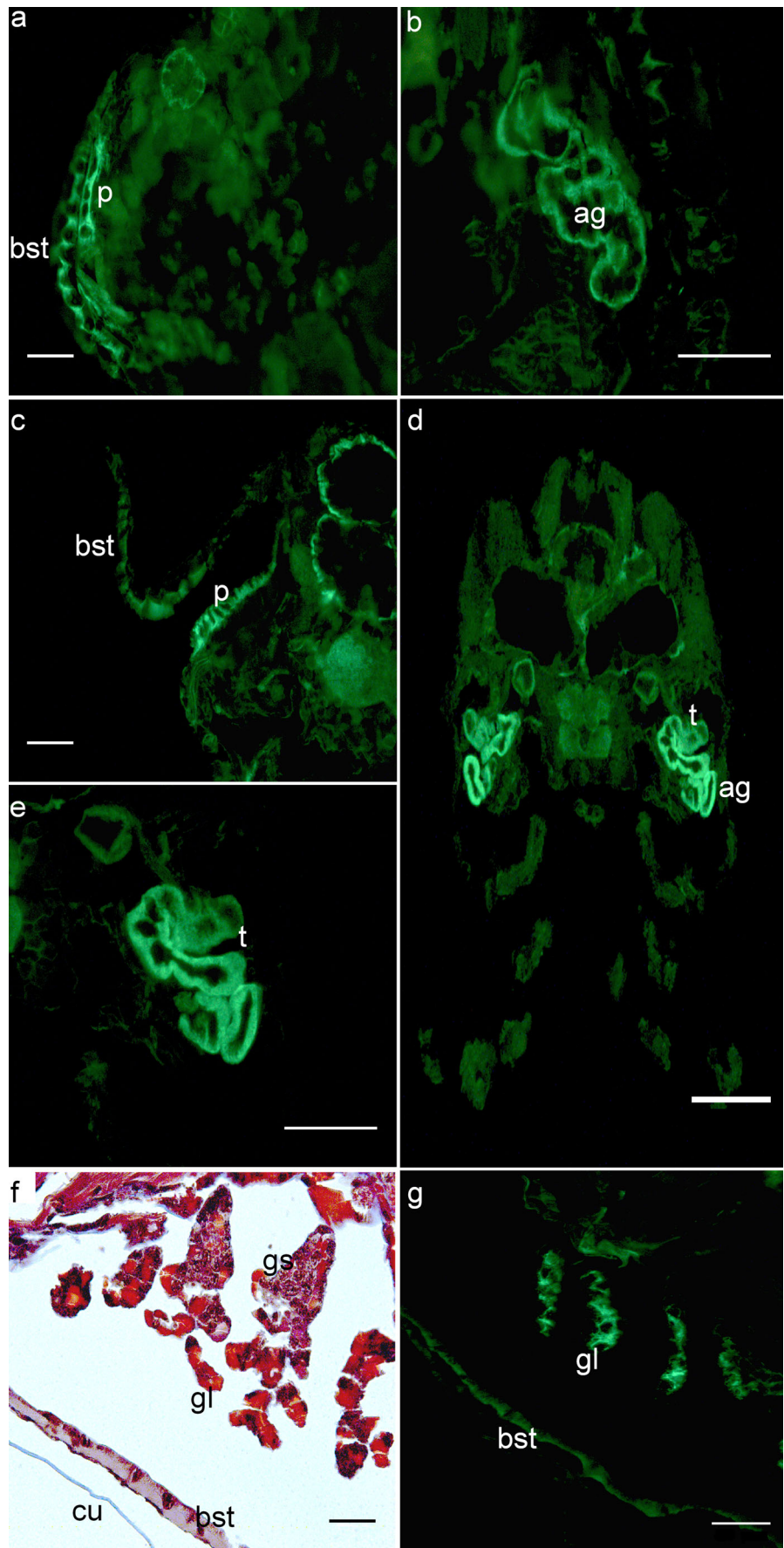
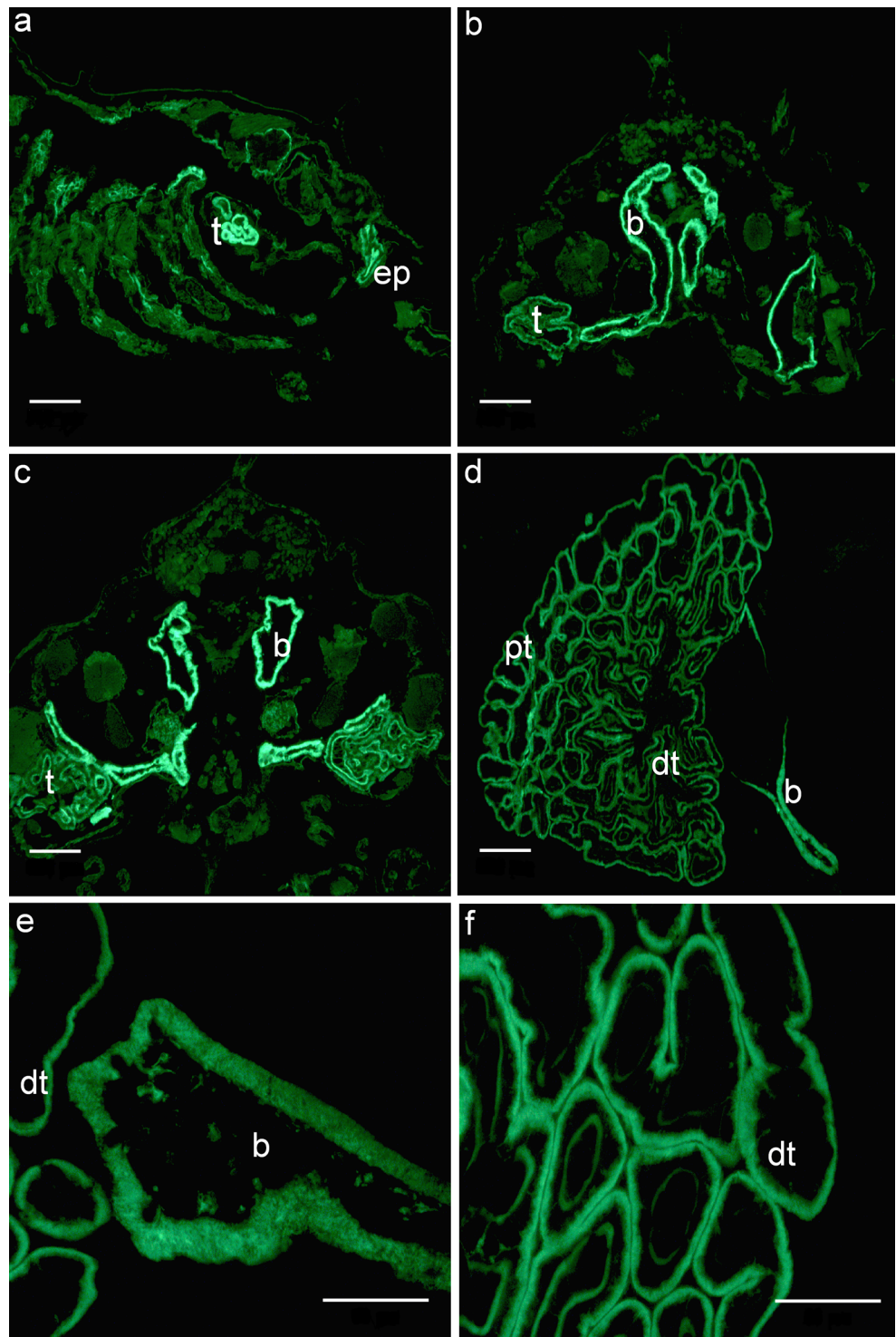


**Fig. 4** Ontogeny of antennal glands in the freshwater shrimp *Palaemonetes argentinus* developed in 1 ‰. **a** Zoea IV stage, longitudinal section. **b** Decapodid stage. **c** Juvenile. **d–f** Adult stage. *b* bladder; *dt* distal tubules; *ep* excretory pore; *pt* proximal tubules; *t* tubules. Scale bars (**a–d**) 300  $\mu$ m; (**e, f**) 50  $\mu$ m



difference in the relative expression of *nka- $\alpha$*  subunit in gills (normalized to Elongation Factor 1- $\alpha$ 1; *efl- $\alpha$ 1*) among salinity treatments (mean  $\pm$  SD, 1 ‰:  $0.59 \pm 0.09$ ; 15 ‰:  $0.63 \pm 0.05$ ; 25 ‰:  $0.54 \pm 0.06$ ;  $F_{2,24} = 0.49$ ;  $P = 0.61$ ). Expression of the housekeeping gene (*efl- $\alpha$ 1*) did not change among salinity treatments ( $F_{2,24} = 2.74$ ;  $P = 0.08$ ).

**Ontogeny** Expression of *nka- $\alpha$*  was detected in all measured samples. Expression of the housekeeping gene (*efl- $\alpha$ 1*) did not change neither throughout ontogeny ( $F_{3,55} = 1.9$ ;  $P = 0.14$ ) nor according to salinities ( $F_{1,55} = 0.198$ ;  $P = 0.51$ ) and there was no interaction between factors ( $F_{3,55} = 0.08$ ;  $P = 0.97$ ). In contrast, *nka- $\alpha$*  (normalized to *efl- $\alpha$ 1* mRNA) was

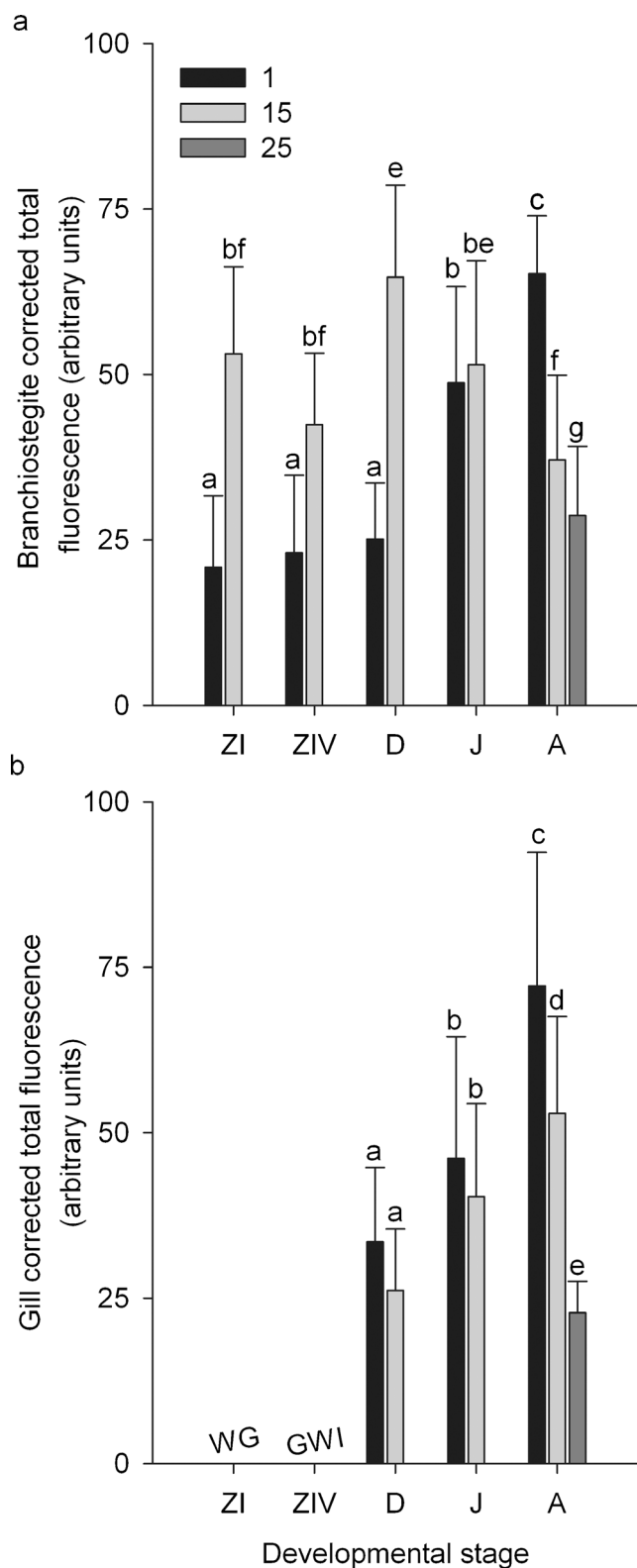


**Fig. 5** Ontogenetic and salinity-induced changes in  $\text{Na}^+/\text{K}^+$ -ATPase (NKA) corrected total fluorescence (CTF) in branchiostegite and gill tissue from *Palaemonetes argentinus*. Larval stages (ZI, ZIV), decapodid (D), juvenile (J) and adult (A). Different letters indicate differences among developmental stages at each level of salinity or between salinities for the same stage ( $P < 0.05$ ). Values: means  $\pm$  SD. WG without gills, GWI gills without immunostaining. 1, 15, 25: salinity in ‰

$P < 0.06$ ). The *nka- $\alpha$*  was already expressed at the earliest embryonic stage (SI), then without change in SII, increasing markedly by 3.7-fold (in 1 ‰) and 5.5-fold (in 15 ‰) at the end of the embryonic development (SIII) and in the first larval stage (ZI) (Fig. 6). Although the pattern of *nka- $\alpha$*  expression during the ontogeny was similar in both salinity treatments, the levels in the SIII and ZI developmental stages were 1.2-fold higher at 15 ‰ than 1 ‰ (Fig. 6).

## Discussion

In the present study, we gathered information about epithelia of *Palaemonetes argentinus* that show significant  $\text{Na}^+/\text{K}^+$ -ATPase expression (as an indicator for tissues with highly active ion-exchange capacities) and the location of NKA throughout ontogeny. As far as we know, this is the first study that shows the location of NKA in extrabranchial embryonic organs from a freshwater palaemonid shrimp.

### Immunolocalization of NKA and ontogeny of osmoregulatory structures

Specialized organs from the branchial chamber are supposed to be involved in the strong ability of *Palaemonetes argentinus* to hyper-osmoregulate in dilute media (Charmantier and Anger 1999). Three different organs from adult branchial chambers (gills, branchiostegites and epipodites) expressed NKA indicating that they are involved in active ion pumping. The presence of NKA in ion-transporting cells of *P. argentinus* gills along with the enhanced gill NKA activity after a salinity challenge (Ituarte et al. 2008) support the prominent role of this organ in active ion exchange. The general organization of the branchial chamber, with a complete branchial formula, is similar in adults and juveniles of *P. argentinus*. As in other palaemonid shrimps, such as *Macrobrachium olfersii*, *M. amazonicum* and *M. rosenbergii* (McNamara and Torres 1999; Boudour-Boucheker et al. 2013; França et al. 2013), gill lamellae of *P. argentinus* juveniles are well developed and show NKA-positive immunoreactivity in the central part of each lamellae. In all the three species of *Macrobrachium*, two different cell types would be linked to active ion transport: the septal cells (that express NKA, as in *P. argentinus*) and the pillar cells (which did not express NKA) located at the border of the

differentially expressed during the ontogeny ( $F_{3,55} = 137.2$ ;  $P < 0.001$ ), between salinities ( $F_{1,55} = 5.9$ ;  $P = 0.018$ ) and there was no interaction between factors ( $F_{3,55} = 2.6$ ;

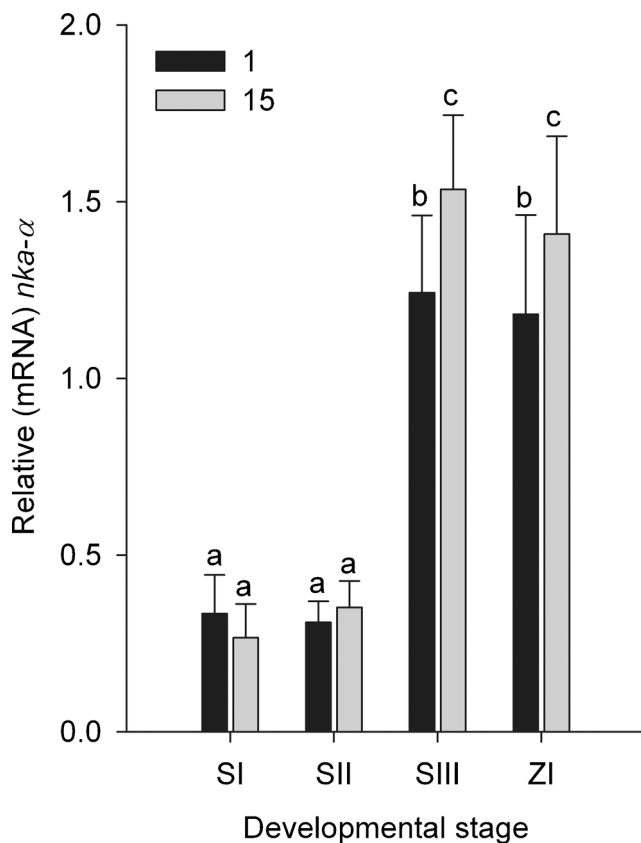


**Fig. 6** Ontogenetic and salinity-induced changes in a relative amount of  $\alpha$ -subunit of  $\text{Na}^+/\text{K}^+$ -ATPase (*nka- $\alpha$* ) mRNA in early developmental stages (whole individuals) from *Palaemonetes argentinus*. Embryonic stages (SI, SII, SIII) and first larvae (ZI). Different letters indicate differences among developmental stages at each level of salinity or between salinities for the same stage ( $P < 0.05$ ). Values: means  $\pm$  SD. 1, 15: salinity in ‰

lamellae (possibly implicated in gas exchange, pH regulation but also ion transport due to the presence of V-type  $\text{H}^+$ -ATPase) (McNamara and Torres 1999; Faleiros et al. 2010; Boudour-Boucheker et al. 2014). The similar NKA distribution suggests a comparable cellular organization in gill lamellae of both freshwater palaemonid species (*M. amazonicum* and *P. argentinus*), which implies that ion transport mechanisms are probably present in two functionally different cell types (Boudour-Boucheker et al. 2014). However, our assumption requires further investigations, notably on the presence of V-type  $\text{H}^+$ -ATPase. It is not to be ruled out that immunopositive cells detected in *P. argentinus* may play a double physiological role in ion uptake and gas exchange (Sousa and Petriella 2005). Unlike crab gills, the structure and NKA immunolabeling of the lamellar epithelium of *P. argentinus* is similar in all lamellae, indicating that each lamella might participate in ion uptake and gas exchange, as has also been reported in other palaemonid shrimps (Martinez et al. 2005; Freire et al. 2008; Faleiros et al. 2010).

The present immunocytochemical study showed that, in late embryos (SIII) and in early larval stages (ZI and ZIV), NKA is located in the inner-side of branchiostegite epithelia,

along pleurae and in antennal glands. The location of ion-transporting tissues is similar to that reported for larvae of other decapods (Felder et al. 1986; Bouaricha et al. 1994; Cieluch et al. 2005), including a palaemonid shrimp (Boudour-Boucheker et al. 2013). As in many decapod larvae, no gills were present in the branchial cavity of first zoea and consequently nor in late embryos. Accordingly, as in *M. amazonicum* from a freshwater population (Charmantier and Anger 2011; Boudour-Boucheker et al. 2013), the capacity of *P. argentinus* to osmoregulate in dilute media (<17 ‰, isotonic point 17 ‰), which is well developed at hatching (Charmantier and Anger 1999), is possibly related to active ion pumping by specialized extrabranchial tissues (branchiostegites, pleurae and antennal glands).

Gill lamellae, still small and under development, are present in the branchial chambers of the ZIV stage but they do not present any specific immunoreactivity for NKA. Developing gills in ZIV are most likely involved in gas exchange (and probably also in other metabolic pathways such as ammonia excretion and pH regulation) rather than in active ion exchange. Gills become fully differentiated at a later life-cycle stage, the decapodid. Specific immunoreactivity indicating the presence of NKA in gills from decapodids has also been recorded in *Macrobrachium amazonicum* (Boudour-Boucheker et al. 2013). In the marine shrimp *Crangon crangon*, unlike the freshwater species *P. argentinus* and *M. amazonicum*, specific immunoreactivity in the gills occurred even later during development, i.e., in the first juvenile stage (Cieluch et al. 2005). The development of fully functional gills may increase the capacity to tolerate low salinities through improved hyperregulation (e.g., Cieluch et al. 2005; Boudour-Boucheker et al. 2013). In *P. argentinus*, however, there is a slight increment in hyper-osmoregulatory capacity in the decapodid compared to earlier zoeal stages. This is consistent with the fact that all life-cycle stages co-occur in habitats where very low salt concentrations prevail and it suggests that extrabranchial organs (including antennal glands) must be extremely efficient for ion exchange until or even during gill development.

Following the postembryonic development of *P. argentinus*, we identified the presence of NKA in branchiostegite epithelial cells, in the two facing epithelia of epipodites and in gills from decapodid, juvenile and adult shrimps; but in all these developmental stages, immunoreactivity was not detected in pleurae (Table 2). A functional shift in the location of osmoregulatory function from pleurae (and branchiostegites) to gills has also been reported in other Caridea such as *Crangon crangon* (Cieluch et al. 2005) and *Macrobrachium amazonicum* (Boudour-Boucheker et al. 2013). Previous studies have shown that branchiostegites, epipodites and pleurae are involved in ion exchange and may be important osmoregulating tissues before gills develop (e.g., Bouaricha et al. 1994; Lignot and Charmantier 2001). Branchiostegites and epipodites

**Table 2** Ontogeny of osmoregulatory structures in *Palaemonetes argentinus*

Developmental stage	Morphological and histological observations	NKA expression	Enzymatic activity	<i>nka-α</i> expression
		Immunolabeling		
Embryonic development	SI Newly fertilized eggs. Majority of egg volume with yolk. Prior gastrula stage.	–	Detectable, but low	Detectable, but low
	SII 50–60 % of egg volume with yolk. Heart is beating. Eyes became visible as reddish lines.	–	Detectable, but low	Detectable, but low
	SIII 5–10 % of egg volume with yolk. Eyes and chromatophores are fully formed. Embryonic movements are observable. Embryos ready to hatch.	Simple tubule-like structures form antennal gland Branchiostegite Pleura	Enhanced values	Enhanced values
Hatching Larval development	ZI Macroscopically visible yolk largely depleted.	Simple tubule-like structures form antennal gland	Lower values than late embryos	Similar values than late embryos
	Natatory exopods on the thoracopodal appendages. Sessile compound eyes.	Branchiostegite Pleura		
	ZIV Stalked compound eyes. Developing gills.	Simple tubule-like structures form antennal gland Branchiostegite Pleura	Not measured	Not measured
	D Gills and one epipodite in each branchial chamber.	Tubules with basal fluorescence and appearance of bladder Branchiostegite Gills and one epipodite in each branchial chamber	Not measured	Not measured
Benthic stages	J Well-formed gill filaments. Benthic stage.	Bladder, proximal and distal tubules Branchiostegites 7 phyllobranchiate gills and 2 small epipodites in each branchial chamber	Not measured	Not measured
	A Well-formed gill filaments. Benthic stage.	Increased size and folding of glands Branchiostegites 7 phyllobranchiate gills and 2 small epipodites in each branchial chamber	Enhanced activity in gills from adults exposed to concentrated salinity during short-term period (48 h)	No detectable change in gene expression in gills from adults exposed to concentrated salinity during long-term period ( $\geq 21$ days)

Summarized data from immunofluorescence light-microscopical observations, gene *nka-α* expression (this study) and NKA enzymatic activity (Ituarte et al. 2008)

appear as the main site of osmoregulation in adults of two caridean species (Martinez et al. 2005) and seem to play a relevant role in *M. amazonicum* juveniles living in fresh water (Boudour-Bouchecker et al. 2013). Hence, these organs (when present) may also contribute to the osmoregulatory capacity of *P. argentinus*.

Increased NKA-corrected total fluorescence (CTF) in gills and branchiostegites during ontogeny in low salinities might provide a good proxy for a higher number of presumptive ion-transporting cells (associated to developing tissues) and/or increased NKA concentration per single cell. An increment in the surface area per unit volume of gill septal cell has been reported for palaemonid freshwater shrimps, suggesting increased membrane availability for insertion of NKA (see McNamara et al. 2015). Thus, NKA concentration may increase in organs from the branchial chamber during the ontogeny of *P. argentinus*. Moreover, more than one NKA  $\alpha$  isoform could be present with different transcription profiles and activation mechanisms. It has been shown that two NKA  $\alpha$  isoforms are expressed in the salt gland and antennal gland of *Artemia franciscana* with development-dependent expression patterns (Escalante et al. 1995). It is likely that different NKA  $\alpha$  isoforms are present in branchiostegites and gills during ontogeny, associated with isoform-specific regulation in transport functions for different physiologic demands, as reported in vertebrates regarding changing salinities (Blanco and Mercer 1998; Deane and Woo 2004).

In addition, we found strong positive immunofluorescence in three regions of the antennal glands (bladder, proximal and distal tubules) in adult *P. argentinus* indicating highly active ion-exchange capacities in this excretory organ. As antennal glands can produce urine, we assume that they are involved in active ion transport from hemolymph filtrate in this shrimp, leading possibly to hypotonic urine as suggested in freshwater crustaceans (Charmantier et al. 2009). As in *Astacus leptodactylus*, we observed higher immunoreactivity in distal than proximal parts of the tubule (especially in the bladder) indicating that distal parts might be the primary site of ion reabsorption in this organ (Khodabandeh et al. 2005). Moreover, NKA staining in the bladder seems to be localized throughout the cells, suggesting deep basal membrane invaginations reaching nearly the apical cell part, while in proximal tubules it seems to be more concentrated on the basal part facing the hemolymph. Although the decapod bladder epithelium participates in absorptive and secretory processes, high levels of NKA may also be related to other non-osmoregulatory transport functions (Khodabandeh et al. 2005; Freire et al. 2008).

#### **Na<sup>+</sup>/K<sup>+</sup>-ATPase $\alpha$ -subunit mRNA expression**

Several studies have previously shown that NKA activity increases prior to hatching in estuarine-dependent decapods

suggesting the occurrence of ion-transporting cells in late embryos (e.g., Felder et al. 1986; Wilder et al. 2001; Taylor and Seneviratna 2005). Enhanced NKA activity in late embryos from *Palaemonetes argentinus* (Ituarte et al. 2008) in correlation with enhanced *nka- $\alpha$*  transcript levels support the assumption that ion-transporting cells from other organs (rather than gills) become functional during the embryonic phase. Likewise, the correlation between low NKA activity and *nka- $\alpha$*  transcript levels from earlier embryonic stages (SI and SII embryos; Ituarte et al. 2008; this study) indicates that extrabranchial organs linked to hyper-osmoregulation may develop at some point about halfway through the embryonic development. Furthermore, enhanced levels of mRNA expression in SIII and ZI developed at higher salinity treatment (15 ‰) suggest that at least part of the increased NKA activity in these early developmental stages after short-term exposure (24 h) at high salinity (Ituarte et al. 2008) could be due to a concomitant rise in the *nka- $\alpha$*  transcript levels. Because the enhanced NKA fluorescence observed in the branchiostegites and antennal glands from larval stages developed at higher salinity, we assume that higher *nka- $\alpha$*  expression in ZI (and possibly in late embryos, SIII) is linked to the NKA located in those epithelia.

It has been shown that NKA expression could change either transiently or permanently, depending on the exposure time after a salinity challenge (e.g., Lovett et al. 2006; Faleiros et al. 2010). For instance, in *Callinectes sapidus*, *nka- $\alpha$*  mRNA levels changed significantly during the process of acclimation to dilute seawater but the transcript quantity returned to initial values after crabs had become fully acclimated to dilute seawater (>18 days; Lovett et al. 2006). In this study, we kept adult shrimps in three different salinities over a long time course ( $\geq 21$  days) but a sudden and short-term exposition (48 h) to increasing salt concentration induced an increase in the NKA activity in isolated gills (Ituarte et al. 2008). Thus, shorter-term alterations in *nka- $\alpha$*  mRNA levels may have been masked due to expression levels returning to initial values. The acclimation of this euryhaline shrimp from fresh water to high salinity concentration (25 ‰) would require that ion-transporting epithelia change from an ion-absorbing to an ion-secreting tissue. Such a reversal of ion pumping mechanisms has been associated with an up-regulation of gill NKA activity in most euryhaline fishes, in which increasing NKA activity is thought to be responsible for regulating plasma Na<sup>+</sup> and Cl<sup>-</sup> levels (Bystriansky et al. 2007). Although immunofluorescence in gills from adult shrimps suggests reduced levels of NKA at higher salinities (fluorescence decreased when salinity increased), whether NKA activity is reduced (or enhanced) at high salinity after long-term acclimation remains to be investigated.

It is believed that the cooperative action of the Na<sup>+</sup>/K<sup>+</sup>-ATPase and at least two other major ion-transporting transmembrane proteins, the V(H<sup>+</sup>)-ATPase and Cl<sup>-</sup>/HCO<sub>3</sub><sup>-</sup>

antiporter, are responsible for ion absorption in palaemonid freshwater shrimps (McNamara and Faria 2012). The current model suggests that the transporters and ion pumps are spatially separated into two different gill cell types (McNamara and Faria 2012; Boudour-Bouchecker et al. 2014; Maraschi et al. 2015). The  $\text{Na}^+/\text{K}^+$ -ATPase activity in the septal cell membranes will likely generate a negative potential difference with respect to the hemolymph that cannot hyperpolarize the apical membrane of the pillar cells. This apical hyperpolarization is likely the result of  $\text{H}^+$  extrusion by the  $\text{V}(\text{H}^+)$ -ATPase into the subcuticular space that will drive inward  $\text{Na}^+$  flux through apical  $\text{Na}^+$  channels. The  $\text{Na}^+/\text{K}^+$ -ATPase activity in the septal cell membranes will transport  $\text{Na}^+$  into the hemolymph from the septal cell cytosol. In *P. argentinus*, as possibly in *Macrobrachium amazonicum*, the capacity to hyperosmoregulate prior and during hatching must depend on extrabranchial organs because there are no gills at this point in development. Future studies should explore if the hyperosmoregulation function is underpinned by molecular mechanisms that involve different  $\text{Na}^+$  pump isozymes (with different profiles of expression) linked to each particular tissue (e.g., Leone et al. 2014). In such a sense, further studies on location and expression of ion-transporting proteins besides NKA could reveal if the current model of transporters is also functional in extrabranchial epithelia during ontogeny of freshwater shrimps.

**Acknowledgments** We wish to thank Ms E. Grousset for valuable assistance with classical histology and Ms E. Blondeau-Bidet for her technical help in molecular biology. This research was supported by PICT 0048–2010 from Agencia Nacional de Promoción Científica y Tecnológica (Argentina) and by a post-doctoral fellowship from Consejo Nacional de Investigaciones Científicas y Técnicas de la República Argentina (CONICET). RBI wishes to thank The Crustacean Society award (2008) and special thanks all the members of AEO team for their assistance.

## References

- Anger K (2001) The biology of decapod crustacean larvae. Crustacean issues 14. Balkema, Lisse
- Blanco G, Mercer RW (1998) Isozymes of the Na-K-ATPase: heterogeneity in structure, diversity in function. Am J Physiol 275:633–650
- Bouaricha N, Charmantier-Daures M, Thuet P, Trilles J-P, Charmantier G (1994) Ontogeny of osmoregulatory structures in the shrimp *Penaeus japonicus* (Crustacea, Decapoda). Biol Bull 186:29–40
- Boudour-Bouchecker N, Boulo V, Lorin-Nebel C, Elguero C, Grousset E, Anger K, Charmantier-Daures M, Charmantier G (2013) Adaptation to freshwater in the palaemonid shrimp *Macrobrachium amazonicum*: comparative ontogeny of osmoregulatory organs. Cell Tissue Res 353:87–98
- Boudour-Bouchecker N, Boulo V, Charmantier-Daures M, Grousset E, Anger K, Charmantier G, Lorin-Nebel C (2014) Differential distribution of V-type  $\text{H}^+$ -ATPase and  $\text{Na}^+/\text{K}^+$ -ATPase in the branchial chamber of the palaemonid shrimp *Macrobrachium amazonicum*. Cell Tissue Res 357:195–206
- Bystriansky JS, Frick NT, Richards JG, Schulte PM, Ballantyne JS (2007) Failure to up-regulate gill  $\text{Na}^+$ ,  $\text{K}^+$ -ATPase  $\alpha$ -subunit isoform  $\alpha 1b$  may limit seawater tolerance of land-locked Arctic char (*Salvelinus alpinus*). Comp Biochem Physiol A 148:332–338
- Charmantier G (1998) Ontogeny of osmoregulation in crustaceans: a review. Invertebr Reprod Dev 33:177–190
- Charmantier G, Anger K (1999) Ontogeny of osmoregulation in the palaemonid shrimp *Palaemonetes argentinus* (Crustacea: Decapoda). Mar Ecol Prog Ser 181:125–129
- Charmantier G, Anger K (2011) Ontogeny of osmoregulatory patterns in the South American shrimp *Macrobrachium amazonicum*: loss of hypo-regulation in a land-locked population indicates phylogenetic separation from estuarine ancestors. J Exp Mar Biol Ecol 396:89–98
- Charmantier G, Charmantier-Daures M (2001) Ontogeny of osmoregulation in crustaceans: the embryonic phase. Am Zool 41:1078–1089
- Charmantier G, Charmantier-Daures M, Towle D (2009) Osmotic and ionic regulation in aquatic arthropods. In: Evans DH (ed) Osmotic and ionic regulation: cells and animals. Taylor & Francis, London, pp 165–208
- Cieluch U, Charmantier G, Grousset E, Charmantier-Daures M, Anger K (2005) Osmoregulation, immunolocalization of  $\text{Na}^+/\text{K}^+$ -ATPase, and ultrastructure of branchial epithelia in the developing brown shrimp, *Crangon crangon* (Decapoda, Caridea). Physiol Biochem Zool 78:1017–1025
- Cieluch U, Anger K, Charmantier-Daures M, Charmantier G (2007) Osmoregulation and immunolocalization of  $\text{Na}^+/\text{K}^+$ -ATPase during the ontogeny of the mitten crab *Eriocheir sinensis* (Decapoda, Grapsoidea). Mar Ecol Prog Ser 329:169–178
- Deane E, Woo NYS (2004) Differential gene expression associated with euryhalinity in sea bream (*Sparus sarba*). Am J Physiol 287:1054–1063
- Escalante R, García-Sáez A, Sastre L (1995) In situ hybridization analyses of Na, K-ATPase  $\alpha$ -subunit expression during early larval development of *Artemia franciscana*. J Histochem Cytochem 43:391–399
- Faleiros RO, Goldman MHS, Furriel RPM, McNamara JC (2010) Differential adjustment in gill  $\text{Na}^+/\text{K}^+$ - and V-ATPase activities and transporter mRNA expression during osmoregulatory acclimation in the cinnamon shrimp *Macrobrachium amazonicum* (Decapoda, Palaemonidae). J Expl Biol 213:3894–3905
- Felder JM, Felder DL, Hand SC (1986) Ontogeny of osmoregulation in the estuarine ghost shrimp *Callinassa jamaicensis* var. *louisianensis* Schmitt (Decapoda, Thalassinidea). J Exp Mar Biol Ecol 99:91–105
- França JL, Pinto MR, Lucena MN, Garçon DP, Valenti WC, McNamara JC, Leone FA (2013) Subcellular localization and kinetic characterization of a gill ( $\text{Na}^+$ ,  $\text{K}^+$ )-ATPase from the giant freshwater prawn *Macrobrachium rosenbergii*. J Membr Biol 246:529–543
- Freire CA, Onken H, McNamara JC (2008) A structure-function analysis of ion transport in crustacean gills and excretory organs. Comp Biochem Physiol 151:272–304
- Ituarte RB (2008) Efectos de la salinidad sobre la reproducción y el desarrollo del camarón de agua dulce *Palaemonetes argentinus*. PhD thesis, Universidad Nacional de Mar del Plata, Mar del Plata
- Ituarte RB, Spivak ED, Anger K (2005) Effects of salinity on embryonic development of *Palaemonetes argentinus* (Crustacea: Decapoda: Palaemonidae) cultured in vitro. Invertebr Reprod Dev 47:213–223
- Ituarte RB, López Mañanes AA, Spivak ED, Anger K (2008) Activity of  $\text{Na}^+$ ,  $\text{K}^+$ -ATPase in a freshwater shrimp, *Palaemonetes argentinus* (Caridea, Palaemonidae): ontogenetic and salinity-induced changes. Aquat Biol 3:283–290
- Ituarte RB, Spivak ED, Camiolo M, Anger K (2010) Effects of salinity on the reproductive cycle of female freshwater shrimp, *Palaemonetes argentinus*. J Crustac Biol 30:186–193

- Johnson KE, Perreau L, Charmantier G, Charmantier-Daures M, Lee CE (2014) Without gills: localization of osmoregulatory function in the copepod *Eurytemora affinis*. *Physiol Biochem Zool* 87:310–324
- Khodabandeh S, Kutnik M, Aujoulat A, Charmantier G, Charmantier-Daures M (2005) Ontogeny of the antennal glands in the crayfish *Astacus leptodactylus* (Crustacea, Decapoda): immunolocalization of  $\text{Na}^+$ ,  $\text{K}^+$ -ATPase. *Cell Tissue Res* 319:167–174
- Khodabandeh S, Charmantier G, Charmantier-Daures M (2006) Immunolocalization of  $\text{Na}^+$ ,  $\text{K}^+$ -ATPase in osmoregulatory organs during the embryonic and post-embryonic development of the lobster *Homarus gammarus*. *J Crustac Biol* 26:515–523
- Lee CE, Bell MA (1999) Causes and consequences of recent freshwater invasions by saltwater animals. *Trends Ecol Evol* 14:284–288
- Lee CE, Kiergaard M, Gelembiuk GW, Eads BD, Posavi M (2011) Pumping ions: rapid parallel evolution of ionic regulation following habitat invasions. *Evolution* 65:2229–2244
- Lee CE, Posavi M, Charmantier G (2012) Rapid evolution of body fluid regulation following independent invasions into freshwater habitats. *J Evol Biol* 25:625–633
- Leone FA, Bezerra TMS, Garçon DP, Lucena MN, Pinto MR, Fontes CFL, McNamara JC (2014) Modulation by  $\text{K}^+$  plus  $\text{NH}_4^+$  of microsomal ( $\text{Na}^+$ ,  $\text{K}^+$ )-ATPase activity in selected ontogenetic stages of the diadromous river shrimp *Macrobrachium amazonicum* (Decapoda, Palaemonidae). *Plos ONE* 9, e89625
- Lignot JH, Charmantier G (2001) Immunolocalization of  $\text{Na}^+$ ,  $\text{K}^+$ -ATPase in the branchial cavity during the early development of the European lobster *Homarus gammarus* (Crustacea, Decapoda). *J Histochem Cytochem* 49:1013–1023
- Lignot JH, Charmantier G (2015) Osmoregulation and excretion (chapter 8). In: Chang E, Thiel M (eds) *Natural history of the Crustacea series, physiological regulation*. Oxford University Press, Oxford
- Lovett DL, Verzi MP, Burgents JE, Tanner CA, Glomski K, Lee JJ, Towle DW (2006) Expression profiles of  $\text{Na}^+$ ,  $\text{K}^+$ -ATPase during acute and chronic hypo-osmotic stress in the blue crab *Callinectes sapidus*. *Biol Bull* 211:58–65
- Lucena MN, Pinto MR, Graçon DP, McNamara JC, Leone FA (2015) A kinetic characterization of the gill  $\text{V}(\text{H}^+)$ -ATPase in juvenile and adult *Macrobrachium amazonicum*, a diadromous palaemonid shrimp. *Comp Biochem Physiol B* 181:15–25
- Lucu C, Towle W (2003)  $\text{Na}^+$ / $\text{K}^+$ -ATPase in gills of aquatic Crustacea. *Comp Biochem Physiol A* 135:195–214
- Maraschi AC, Freire CA, Prodocimo V (2015) Immunocytochemical localization of  $\text{V-H}^+$ -ATPase,  $\text{Na}^+$ / $\text{K}^+$ -ATPase, and carbonic anhydrase in gill lamellae of adult freshwater euryhaline shrimp *Macrobrachium acanthurus* (Decapoda, Palaemonidae). *J Exp Zool* 9999A:1–8
- Martinez AS, Charmantier G, Compère P, Charmantier-Daures M (2005) Branchial chamber tissues in two caridean shrimps: the epibenthic *Palaemon adspersus* and the deep-sea hydrothermal *Rimicaris exoculata*. *Tissue Cell* 37:153–165
- McNamara JC, Faria SC (2012) Evolution of osmoregulatory patterns and gill ion transport mechanisms in the decapods Crustacea: a review. *J Comp Physiol B* 182:997–1014
- McNamara JC, Torres AH (1999) Ultracytochemical location of  $\text{Na}^+$ / $\text{K}^+$ -ATPase activity and effect of high salinity acclimation in gill and renal epithelia of the freshwater shrimp *Macrobrachium olfersii* (Crustacea, Decapoda). *J Exp Zool* 284:617–628
- McNamara JC, Freire CA, Torres AH Jr, Faria SC (2015) The conquest of fresh water by the palaemonid shrimps: an evolutionary history scripted in the osmoregulatory epithelia of the gills and antennal glands. *Biol J Linn Soc* 114:673–688
- Menú-Marque SA (1973) Desarrollo larval de *Palaemonetes argentinus* (Nobili, 1901) en el laboratorio (Crustacea, Caridea, Palaemonidae). *Physis* 32:149–169
- Miller MF, Labandeira CC (2002) Slow crawl across the salinity divide: delayed colonization of freshwater ecosystems by invertebrates. *GSA Today* 12:4–10
- Péqueux A (1995) Osmotic regulation in crustaceans. *J Crustac Biol* 15:1–60
- Robertson S (2013) The dorsal organ: what is it and what is it for? *Plymouth Student Scientist* 6:412–422
- Seneviratna D, Taylor HH (2006) Ontogeny of osmoregulation in embryos of intertidal crabs (*Hemigrapsus sexdentatus* and *H. crenulatus*, Grapsidae, Brachyura): putative involvement of the embryonic dorsal organ. *J Exp Biol* 209:1487–1501
- Sousa LG, Petriella AM (2005) Gill morphology and ultrastructure of the prawn, *Palaemonetes argentinus* Nobili, 1901 (Decapoda, Caridea). *Crustaceana* 78:409–420
- Susanto GN, Charmantier G (2000) Ontogeny of osmoregulation in the crayfish *Astacus leptodactylus*. *Physiol Biochem Zool* 73:169–176
- Susanto GN, Charmantier G (2001) Crayfish freshwater adaptation starts in eggs: ontogeny of osmoregulation in embryos of *Astacus leptodactylus*. *J Exp Zool* 289:433–440
- Taylor HH, Seneviratna D (2005) Ontogeny of salinity tolerance and hyper-osmoregulation by embryos of the intertidal crabs *Hemigrapsus edwardsii* and *Hemigrapsus crenulatus* (Decapoda, Grapsidae): survival of acute hyposaline exposure. *Comp Biochem Physiol A* 140:495–505
- Weihrauch D, Ziegler A, Siebers D, Towle DW (2001) Molecular characterization of Vtype  $\text{H}^+$ -ATPase (B subunit) in gill of euryhaline crab and its physiological role in osmoregulatory ion uptake. *J Exp Biol* 204:25–37
- Weihrauch D, McNamara JC, Towle D, Onken H (2004) Ion-motive ATPases and active transbranchial  $\text{NaCl}$  uptake in the red freshwater crab *Dilocarcinus pagei* (Decapoda, Trichodactylidae). *J Exp Biol* 207:4623–4631
- Wilder MN, Huong DTT, Okuno A, Atmomarsono M, Yang W-J (2001) Oubain-sensitive  $\text{Na/K}$ -ATPase activity increases during embryogenesis in the giant freshwater prawn *Macrobrachium rosenbergii*. *Fish Sci* 67:182–184